Inorganic Chemistry

Article

pubs.acs.org/IC

Novel Fundamental Building Blocks and Site Dependent Isomorphism in the First Actinide Borophosphates

Shijun Wu,[†,‡,§] Matthew J. Polinski,[∥] Thomas Malcherek,[⊥] Ulrich Bismayer,[⊥] Martina Klinkenberg,[§] Giuseppe Modolo,[§] Dirk Bosbach,[§] Wulf Depmeier,[‡] Thomas E. Albrecht-Schmitt,*[,∥,#] and Evgeny V. Alekseev*[,§,▽]

[†]Guangzhou Institute of Geochemistry, Chinese Academy of Sciences, 511 Kehua Street, 510640 Guangzhou, P. R. China

[‡]Institut für Geowissenschaften, Universität zu Kiel, 24118 Kiel, Germany

[§]Institute for Energy and Climate Research (IEK-6), Forschungszentrum Jülich GmbH, 52428 Jülich, Germany

[∥]Department of Civil Engineering and Geological Sciences and Department of Chemistry and Biochemistry, University of Notre Dame, 156 Fitzpatrick Hall, Notre Dame, Indiana 46556, United States

[⊥]Mineralogisch-Petrographisches Institut, Universität Hamburg, Grindelallee 48, 20146 Hamburg, Germany

[#]Department of Chemistry and Biochemistry, Florida State University, 102 Varsity Way, Tallahassee, Florida 32306-4390, United States

[▽]Institut für Kristallographie, RWTH Aachen University, 52066 Aachen, Germany

Supporting Information

ABSTRACT: Three novel uranyl borophosphates, $Ag_2(NH_4)_3[(UO_2)_2\{B_3O(PO_4)_4(PO_4H)_2\}]H_2O$ (**AgNBPU-1**), $Ag_{(2-x)}(NH_4)_3[(UO_2)_2\{B_2P_5O_{(20-x)}(OH)_x\}]$ (x = 1.26) (**AgNBPU-2**), and $Ag_{(2-x)}(NH_4)_3[(UO_2)_2\{B_2P_{(5-y)}As_yO_{(20-x)}(OH)_x\}]$ (x = 1.43, y = 2.24) (**AgNBPU-3**), have been prepared by the H_3BO_3–$NH_4H_2PO_4/NH_4H_2AsO_4$ flux method. The structure of **AgNBPU-1** has an unprecedented fundamental building block (FBB), composed of three BO_4 and six PO_4 tetrahedra which can be written as 9□:[Φ] □⟨3□⟩□|□⟨3□⟩□|□⟨3□⟩□|. Two Ag atoms are linearly coordinated; the coordination of a third one is T-shaped. **AgNBPU-2** and **AgNBPU-3** are isostructural and possess a FBB of two BO_4 and five TO_4 (T = P, As) tetrahedra (7□:□⟨4□⟩□|□). **AgNBPU-3** is a solid solution with some PO_4 tetrahedra of the **AgNBPU-2** end-member being substituted by AsO_4. Only two out of the three independent P positions are partially occupied by As, resulting in site dependent isomorphism. The three compounds represent the first actinide borophosphates.

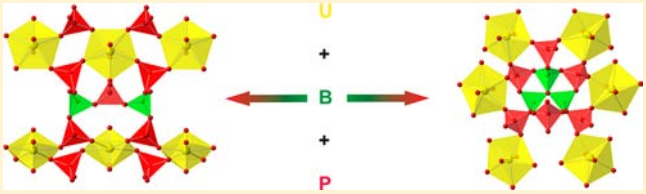

1. INTRODUCTION

Borophosphates are ternary or multinary oxide compounds in M_xO_y–B_2O_3–P_2O_5–(H_2O) systems containing complex anionic partial structures built of borate (BO_4, BO_3) and phosphate (PO_4) groups, or their partially protonated derivatives.[1] The term "borophosphate" is used to denote phases in which borate groups are directly connected with phosphate groups. Compounds containing isolated borate and phosphate groups are referred to as "borate-phosphate".[2] Only two minerals are known which contain borate and phosphate groups as the main anions, viz. lüneburgite (a borophosphate)[3] and seamanite (a borate-phosphate).[4] In recent years, several new borate-containing minerals have been reported in which some phosphate exists as a minor component. These minerals include byzantievite,[5] proshchenkoite,[6] hundholmenite,[7] okanoganite-(Y),[8] and vicanite-(Ce).[9] While the first study of borophosphate was conducted almost 150 years ago,[10] systematic research on crystalline borophosphates has been performed during the past 18 years.[11] Since then, hundreds of borophosphate compounds have been reported and reviewed.[1,11]

Besides crystals, borophosphate glasses have found high interest owing to their various real or potential technological applications, such as their use as bone transplantates,[12] solid-state lasers,[13] sealant,[14] even nonlinear optical devices if suitably poled,[15] and matrix for nuclear waste vitrification.[16] The last point has generated some concern since during long-term storage and under certain circumstances nuclear waste glasses might undergo corrosion with subsequent formation of numerous crystalline products and possible degradation of the mechanical integrity of the glass.[17] Of the numerous uranyl phosphate minerals observed in nature, probably the best-known is autunite.[18] It has been shown that autunite can also form as an alteration product of spent nuclear fuel.[19] In order to know which crystalline products may possibly occur in corroded nuclear waste, numerous actinide phosphates[20,21]

Received: January 28, 2013
Published: July 3, 2013

   dx.doi.org/10.1021/ic400214x | *Inorg. Chem.* 2013, 52, 7881–7888

and actinide borates[22,23] have been prepared in systems relevant to nuclear waste. It was only recently that actinide compounds containing both borate and phosphate groups became known, viz. the borate-phosphates $Th_2(BO_4)(PO_4)$[24] and $Ba_5[(UO_2)(PO_4)_3(B_5O_9)]\cdot nH_2O$.[25] These compounds were prepared by high temperature solid state reactions. However, the knowledge of actinide borophosphate is scarce up to now. In order to explore the world of actinide borophosphate, we adopted boric acid together with phosphate salt as the reactive flux. Therefore, the first actinide borophosphates, $Ag_2(NH_4)_3[(UO_2)_2\{B_3O(PO_4)_4(PO_4H)_2\}]\cdot H_2O$ (**AgNBPU-1**), $Ag_{(2-x)}(NH_4)_3[(UO_2)_2\{B_2P_5O_{(20-x)}(OH)_x\}]$ (x = 1.26) (**AgNBPU-2**), and $Ag_{(2-x)}(NH_4)_3[(UO_2)_2\{B_2P_{(5-y)}As_yO_{(20-x)}(OH)_x\}]$ (x = 1.43, y = 2.24) (**AgNBPU-3**), were synthesized and reported here. Both **AgNBPU-1** and **AgNBPU-2** show new borophosphate motives. **AgNBPU-1** contains an unusual B_3O_{10} group in which three BO_4 tetrahedra are connected to each other by sharing a common vertex. **AgNBPU-3** is isomorphous with **AgNBPU-2** with about 50% substitution of As for P. The crystal structures, infrared spectra, and UV−vis−NIR spectra of all compounds are reported.

2. EXPERIMENTAL SECTION

2.1. Syntheses. $UO_2(NO_3)_2\cdot 6H_2O$(Merck), $AgNO_3$(Rudolf Walter), $NH_4H_2PO_4$(Alfa-Aesar), $NH_4H_2AsO_4$(Alfa-Aesar), H_3PO_4(85%, Alfa-Aesar), and H_3BO_3 (Alfa-Aesar) were used as received. ***Caution!*** *The $UO_2(NO_3)_2\cdot 6H_2O$ used in this study contained depleted uranium; standard precautions for handling radioactive materials should be followed.*

*$Ag_2(NH_4)_3[(UO_2)_2\{B_3O(PO_4)_4(PO_4H)_2\}]H_2O$ (**AgNBPU-1**).* $AgNO_3$ (84.94 mg), H_3BO_3 (97.07 mg), H_3PO_4 (216 μL), $NH_4H_2PO_4$ (517.64 mg), $UO_2(NO_3)_2\cdot 6H_2O$ (125.53 mg), and 50 μL of deionized water were loaded into a 60 mL PTFE-lined autoclave. The molar ratio for the reactants was $AgNO_3$:H_3BO_3:H_3PO_4:$NH_4H_2PO_4$:$UO_2(NO_3)_2\cdot 6H_2O$ = 2:6:12.6:18:1. The autoclave was sealed and heated up to 200 °C within 2 h in a box furnace and held at 200 °C for 72 h, and then cooled to room temperature at a rate of 7 °C/h. The resulting product was washed with hot water to remove excess boric acid and $NH_4H_2PO_4$, followed by rinsing with ethanol. Green yellow prismatic or needle-shaped crystals were collected for further measurement. There are some pale white amorphous byproducts always present (confirmed by microscope observation) which cannot be removed by washing.

*$Ag_{(2-x)}(NH_4)_3[(UO2)_2\{B_2P_5O_{(20-x)}(OH)_x\}]$ (x = 1.26) (**AgNBPU-2**).* The only difference with the preparation of **AgNBPU-1** was the lower amount of $NH_4H_2PO_4$, but higher amount of $UO_2(NO_3)_2\cdot 6H_2O$, such that the molar ratio was 2:6:12.6:12:2. Apart from this the experimental conditions were identical. Pale yellow prismatic or needle-shaped crystals were collected for further measurement. There are some pale white amorphous byproducts always present (confirmed by microscope observation) which cannot be removed by washing.

*$Ag_{(2-x)}(NH_4)_3[(UO_2)_2\{B_2P_{(5-y)}As_yO_{(20-x)}(OH)_x\}]$ (x = 1.43, y = 2.24) (**AgNBPU-3**).* The preparation of **AgNBPU-3** was again performed under identical conditions as before, with the exception that $NH_4H_2PO_4$ was replaced by $NH_4H_2AsO_4$. Pale green prismatic or needle-shaped crystals were obtained and chosen for subsequent characterization.

2.2. EDX Analysis. For the determination of the chemical composition of the samples, an environmental scanning electron microscope FEI Quanta 200F with Genesis (EDAX) EDS-system was used. The measurements were carried out in low-vacuum mode at 0.6 mbar (20 kV, spot size 4, working distance 10 mm). When using this mode, sputtering of the samples with gold or carbon is not necessary, and artifacts are avoided. The samples were prepared as powders/grains on adhesive carbon tabs.

2.3. Crystallographic Studies. Crystals selected for data collection were mounted on a Nonius CCD four circle diffractometer. All data were collected using monochromatic Mo Kα radiation (λ = 0.710 73 Å). More than one hemisphere of data was collected for each crystal, and the three-dimensional (3D) data were integrated and corrected for Lorentz, polarization, and background effects using the Eval14 procedures[26] as implemented in the supporting programs for the diffractometer. Data were scaled and corrected for absorption effects using SADABS.[27] Additional information pertinent to the data collection is given in Table 1. The SHELXL-97 program[28] was used for the determination and refinement of the structures. The structures were solved by direct methods and refined to R_1 = 0.0461 for **AgNBPU-1**, 0.0390 for **AgNBPU-2**, and 0.0694 for **AgNBPU-3**.

Table 1. Crystallographic Data for $Ag_2(NH_4)_3[(UO_2)_2\{B_3O(PO_4)_4(PO_4H)_2\}]H_2O$ (AgNBPU-1), $Ag_{(2-x)}(NH_4)_3[(UO_2)_2\{B_2P_5O_{(20-x)}(OH)_x\}]$ (x = 1.26) (AgNBPU-2), and $Ag_{(2-x)}(NH_4)_3[(UO_2)_2\{B_2P_{(5-y)}As_yO_{(20-x)}(OH)_x\}]$ (x = 1.43, y = 2.24) (AgNBPU-3)

	AgNBPU-1	AgNBPU-2	AgNBPU-3
color and habit	green-yellow, prism	pale-yellow, prism	pale-green, prism
crystal system	triclinic	orthorhombic	orthorhombic
space group	$P\bar{1}$	*Pcmn*	*Pcmn*
a (Å)	8.506(2)	12.011(4)	12.109(3)
b (Å)	9.282(1)	12.166(3)	12.353(6)
c (Å)	17.508(5)	14.454(4)	14.678(4)
α (deg)	90.37(2)	90	90
β (deg)	89.71(2)	90	90
γ (deg)	104.56(2)	90	90
V (Å^3)	1337.9(5)	2112.0(11)	2195.7(13)
Z	2	4	4
T (K)	293(2)	293(2)	293(2)
λ (Å)	0.710 73	0.710 73	0.710 73
reflns collected	36 672	57 345	70 895
indep reflns	6652	2857	2854
indep reflns with $I > 2\sigma(I)$	5688	2437	2633
max 2θ (deg)	56.56	56.56	56.56
ρ_{calcd} (g cm^{-3})	3.555	3.643	3.747
μ (Mo K) (cm^{-1})	140.02	164.82	188.94
$R(F)$ for $F_o^2 > 2(F_o^2)^a$	0.0461	0.0390	0.0703
$R_w(F_o^2)^b$	0.1198	0.0834	0.1596
GOF^c	1.041	1.121	1.360

$^aR(F) = \sum||F_o| - |F_c||/\sum|F_o|$. $^bR(F_o^2) = [w(F_o^2 - F_c^2)^2/\sum w(F_o^4)]^{1/2}$. ^{c}GOF = goodness of fit.

2.4. Infrared Spectroscopy. Infrared spectra were obtained from single crystals using a SensIR technology IlluminatIR FT-IR microspectrometer. Single crystals were placed on quartz IR slides, and the spectrum was collected with a diamond ATR objective. Each spectrum was acquired from 650 to 4000 cm^{-1} with a beam aperture of 100 mm.

2.5. UV−Vis−NIR Spectroscopy. UV−vis−NIR spectra data were obtained from single crystals using a Craic Technologies UV−vis−NIR microspectrophotometer. Crystals were placed on quartz slides under Krytox oil, and the data were collected from 500 to 1400 nm. The exposure time was auto-optimized by the Craic software.

3. RESULTS AND DISCUSSION

3.1. Syntheses. Crystal growth from high-temperature solutions (flux method) is commonly used for the preparation of single crystals. $NH_4H_2PO_4$ (melting point, 190 °C) has been used as a flux.[29] In some cases, a mixture of H_3BO_3 and $NH_4H_2PO_4$ was used to prepare borophosphates.[30] In the

dx.doi.org/10.1021/ic400214x | Inorg. Chem. 2013, 52, 7881−7888

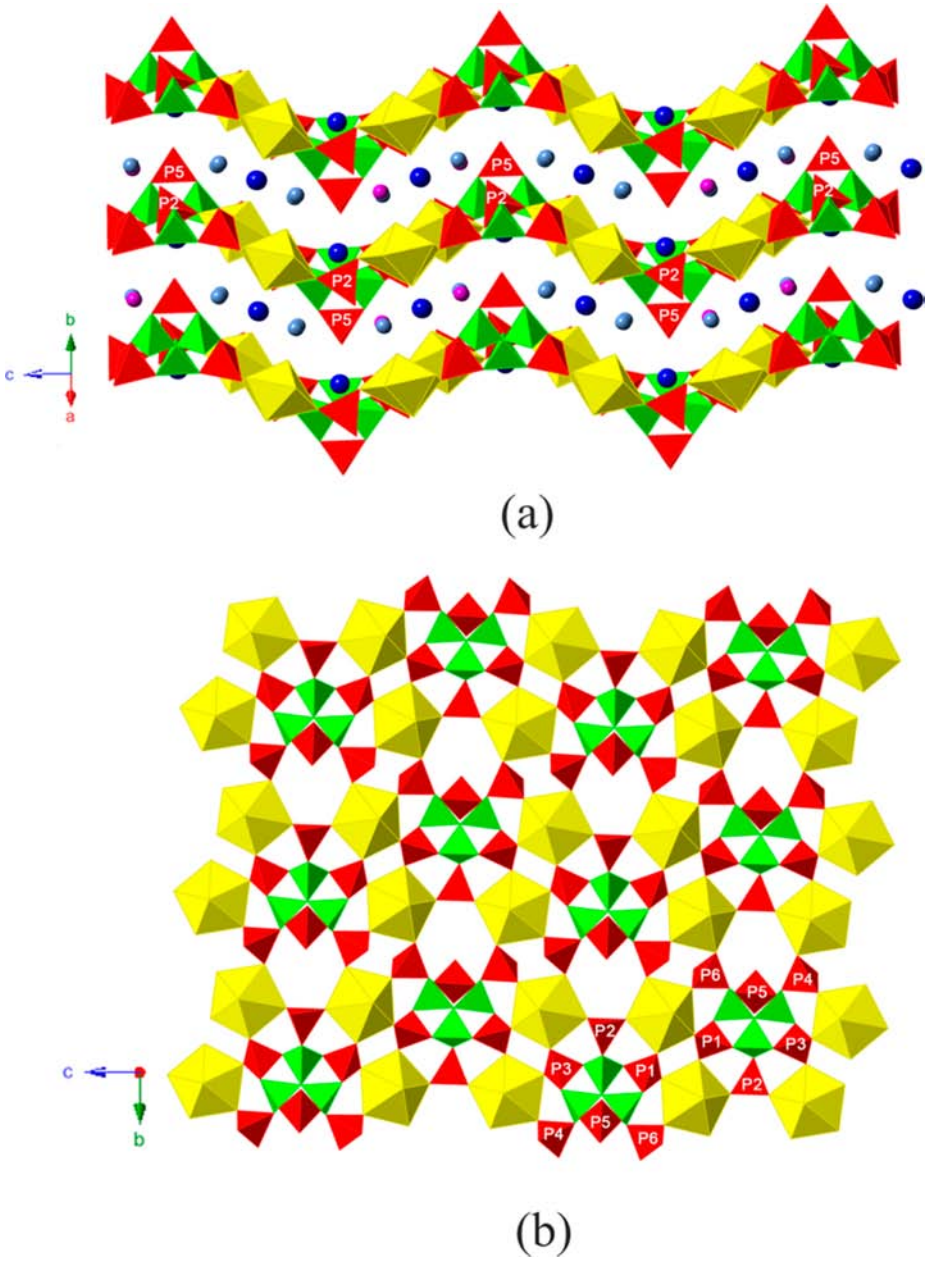

Figure 1. Polyhedral view of the structure of **AgNBPU-1** (a) and its 2D layer extends in the *bc*-plane (b). UO_7 pentagonal bipyramids are shown in yellow, BO_4 tetrahedra are shown in green, PO_4 tetrahedra are shown in red. Ag atoms are shown in blue, NH_4^+ groups are shown in pale blue, and water molecules are shown in violet spheres, respectively.

present study, the H_3BO_3–$NH_4H_2PO_4$ flux method was used to prepare the first actinide borophosphates.

Our experiments have shown that the stoichiometric ratio of the reactants is crucial for the success of crystal growth and for the question of which phase is formed. **AgNBPU-2** can only form when the ratio of $AgNO_3$:H_3BO_3:H_3PO_4:$NH_4H_2PO_4$:$UO_2(NO_3)_2{\cdot}6H_2O$ is 2:6:12.6:12:2, or when the uranium content is higher than 2. With less U (e.g., $AgNO_3$:H_3BO_3:H_3PO_4:$NH_4H_2PO_4$:$UO_2(NO_3)_2{\cdot}6H_2O$ = 2:6:12.6:12:1), only an amorphous phase was observed. On the contrary, when more U was used (e.g., $AgNO_3$:H_3BO_3:H_3PO_4:$NH_4H_2PO_4$:$UO_2(NO_3)_2{\cdot}6H_2O$ = 2:6:12.6:12:3), the yield of **AgNBPU-2** was higher which was decided through microscope observation. When $NH_4H_2PO_4$ was replaced by $NH_4H_2AsO_4$, **AgNBPU-3** was obtained. Wang et al. have demonstrated that varying the initial amount of flux (which acts also as a reactant) can induce different phases.[23] As regards the experimental conditions, the syntheses of **AgNBPU-1** and **AgNBPU-2** are identical, except for the different stoichiometric ratios of the reactants. When more $NH_4H_2PO_4$ was used ($AgNO_3$:H_3BO_3:H_3PO_4:$NH_4H_2PO_4$:$UO_2(NO_3)_2{\cdot}6H_2O$ = 2:6:12.6:18:1), only **AgNBPU-1** is formed. Furthermore, when H_3PO_4 was absent, only **AgNBPU-1** was observed in all reactions even if the other reactants were in the same ratio as for **AgNBPU-2** (Table S1). As a matter of fact **AgNBPU-2** can be synthesized only in the presence of H_3PO_4 which implies that its nucleation process and/or crystal growth mechanism might require specific low pH values as compared with **AgNBPU-1**.

dx.doi.org/10.1021/ic400214x | *Inorg. Chem.* 2013, 52, 7881–7888

The EDX data shows that the ratios of P:Ag:U is 5.55:2.10:2.00 for **AgNBPU-1** and 4.71:0.71:2.00 for **AgNBPU-2**, respectively. And the ratio of P:As:Ag:U is 3.34:2.76:0.86:2.00 for **AgNBPU-3**. All these detected ratios are close to the ideal one (Table S2−S4). The SEM images demonstrate that the crystal surface of **AgNBPU-1** is much more clear compared with **AgNBPU-2** and **AgNBPU-3** (Figure S4−S6).

3.2. Structural Features. *$Ag_2(NH_4)_3[(UO_2)_2\{B_3O(PO_4)_4(PO_4H)_2\}]H_2O$.* A polyhedral view of the structure of **AgNBPU-1** is shown in Figure 1a. The structure is based on corrugated 2D layers with complex compositions. A top view of the layer is presented in Figure 1b. The layers are constructed from complex borophosphate finite clusters linked by $(UO_2)^{2+}$ uranyl groups. The uranyl groups are coordinated by five oxygen atoms resulting in pentagonal bipyramidal (UO_7) coordination of the two crystallographically independent uranium atoms. The bond lengths in the uranyl groups are in the range from 1.753(9) to 1.797(11) Å. As expected, the equatorial U−O bond lengths are significantly longer and range from 2.312(11) to 2.466(10) Å. Bond valence sum (BVS) analysis confirms the presence of U^{6+} in both crystallographic positions (Table S12).[31]

In each layer, the uranyl groups are surrounded by complex oxo-borophosphate clusters. The core of these clusters is based on three tetrahedral BO_4 groups (Figure 1b). The tetrahedra are linked via μ_3 oxygen atoms forming a propeller-like geometry ($[O^{[3]}(B^{[4]}O_3^{[2]})_3]^{11-}$). The same type of polyborate cluster has been observed in both trivalent lanthanide[32] and actinide (Pu, Am, Cm) borates,[22c−g] but here we report on such a polyborate cluster in compounds with a higher oxidation state of the actinide (U^{6+}). A similar geometry has also been observed in compounds with other elements in tetrahedron centers, for example in zinc phosphate.[33] The bond lengths in the BO_4 groups are quite normal and range from 1.42(2) to 1.569(11) Å. The oxo-borate tetrahedra are surrounded only by P atoms and do not have direct contacts with the uranyl groups. There are six symmetrically independent positions for the P atoms, all of which form PO_4 tetrahedra and are linked by corner-sharing oxygen atoms with the other groups within the layers. Two of these groups (P1, P3) do not have terminal P−O bonds and are fully coordinated by uranyl and oxo-borate groups. The BVS calculations show that these groups do not contain OH groups and are thus pure orthophosphate.[31] Three PO_4 groups (P2, P4, P6), have one terminal P−O bond (Figure 1b), one of which, ($P(2)O_4$), is a hydroxylated (PO_3OH) group as determined by BVS calculation.[31] The last group around P(5) shares only two oxygens with the oxo-borate cluster, and the two terminal P−O bonds point into the interlayer space. According to BVS, one of these oxygen atoms, O22, is protonated making it the second (PO_3OH) group in this structure.[31]

Two of the three Ag^+ cations, Ag2 and Ag3, reside between the uranyl borophosphate layers as shown in Figure 1a. Both Ag2 and Ag3 are in 2-fold linear coordination with Ag2−O19 and Ag3−O23 distances of 2.21(1) and 2.19(1) Å, respectively (Table S6). This kind of coordination is well-known for Ag(I).[34] Since both Ag atoms occupy a position on the inversion center, the two bonds at each Ag are equivalent and the corresponding angle O−Ag−O is 180° by symmetry. Ag1 is on a general position and is 3-fold T-shaped coordinated with Ag−O distances between 2.36 (1) and 2.41(1) Å (Table S6). T-shaped coordinated Ag are not so common but also have been reported in crystalline compounds.[35] Two of these atoms (O20, O25) belong to neighboring layers, and O20−Ag−O25 spans the interlayer. The angle O20−Ag−O25 is almost straight (171.9(3)°). The third O atom in this coordination, O21, belongs to the same layer as O20. The angles O21−Ag−O20 and O21−Ag−O25 are slightly larger than 90° (Table S7). The formula of the layers can be written as $[(UO_2)_2\{B_3O(PO_4)_4(PO_4H)_2\}]_2^{5-}$. Water molecules and ammonium occupy the interlayer space which has been confirmed by the IR spectrum as shown in Figure S8 and Table S5. The quantity of ammonium is determined according to the charge balance requirement. Finally, oxygen and nitrogen in water and ammonium molecules were distinguished according to the R_1 value during the structure refinement.

From Figure 1 and Table 1 it is obvious that the structure of **AgNBPU-1** is strongly pseudosymmetric with pseudomonoclinic mirror planes perpendicular to the *c*-axis. The main deviation from monoclinicity is shown by the hydroxylated $P(2)O_3OH$ groups, which are tilted away from the mirror plane, and concomitant shifts of the uranyl polyhedra linked to them. It implies that the strong pseudosymmetric **AgNBPU-1** might eventually transform into a real monoclinic structure with dehydration or dehydroxylation at higher temperature.

*$Ag_{(2-x)}(NH_4)_3[(UO_2)_2\{B_2P_{(5-y)}As_yO_{(20-x)}(OH)_x\}]$ ($x = 1.26$, $y = 0$ for **AgNBPU-2** and $x = 1.43$, $y = 2.24$ for **AgNBPU-3**).* **AgNBPU-2** and **AgNBPU-3** are isostructural, and only the pure borophosphate **AgNBPU-2** will be discussed in order to describe their main structural features. The structure of this phase is a complex 3D framework presented in Figure 2a. The framework is based on 1D borophosphate chains with complex geometry (Figure 2c) linked by UO_2^{2+} uranyl groups. The uranium atoms (UO_7) have pentagonal bipyramidal coordination geometry. The U−O bond lengths are in the range from 1.755(7) to 1.802(8) Å for the uranyl groups and 2.314(4) to 2.409(4) Å for the oxygens in the equatorial plane. These bond lengths are as expected for U^{6+} phases. The corrugated periodically repeatable layer-like fragment (Figure 2b) can be separated from the 3D framework as emphasized using blue background in Figure 2a. From this fragment one can see that each U center is surrounded by five PO_4 groups via corner-sharing (Figure 2b). There are three symmetrically independent PO_4 and one symmetrically independent BO_4 groups in this structure. The BO_4 tetrahedron shares corners with four neighboring PO_4 tetrahedra, three of which belong to the same corrugated layer, whereas the fourth joins these layers in the *c*-direction.

The B−O bond lengths within the BO_4 tetrahedra range from 1.439(7) to 1.480(7) Å. The BO_4 tetrahedra are surrounded by four PO_4 groups and play a prime role in the building of the borophosphate chain (Figure 2c). Of the three symmetrically independent P atoms, two (P1, P3) are PO_4 orthophosphate groups fully bonded to two BO_4 and two UO_2^{2+} groups. The P−O bond lengths range from 1.501(4) to 1.574(5) Å. The third PO_4 group (P2) has one terminal P−O bond (P2−O10) directed into the channel space. The BVS calculation shows that this site can be partially occupied by a hydroxyl group.[31] This might explain the nonstoichiometric presence of Ag in the structures of both phases. The borophosphate chain is parallel to *b*-axis and has a complex form (Figure 2c). The geometry of the chain is adopted to chelate linear uranyl groups. Each unit (separated in Figure 2c) of the borophosphate chain chelates four uranyl groups.

dx.doi.org/10.1021/ic400214x | *Inorg. Chem.* 2013, 52, 7881−7888

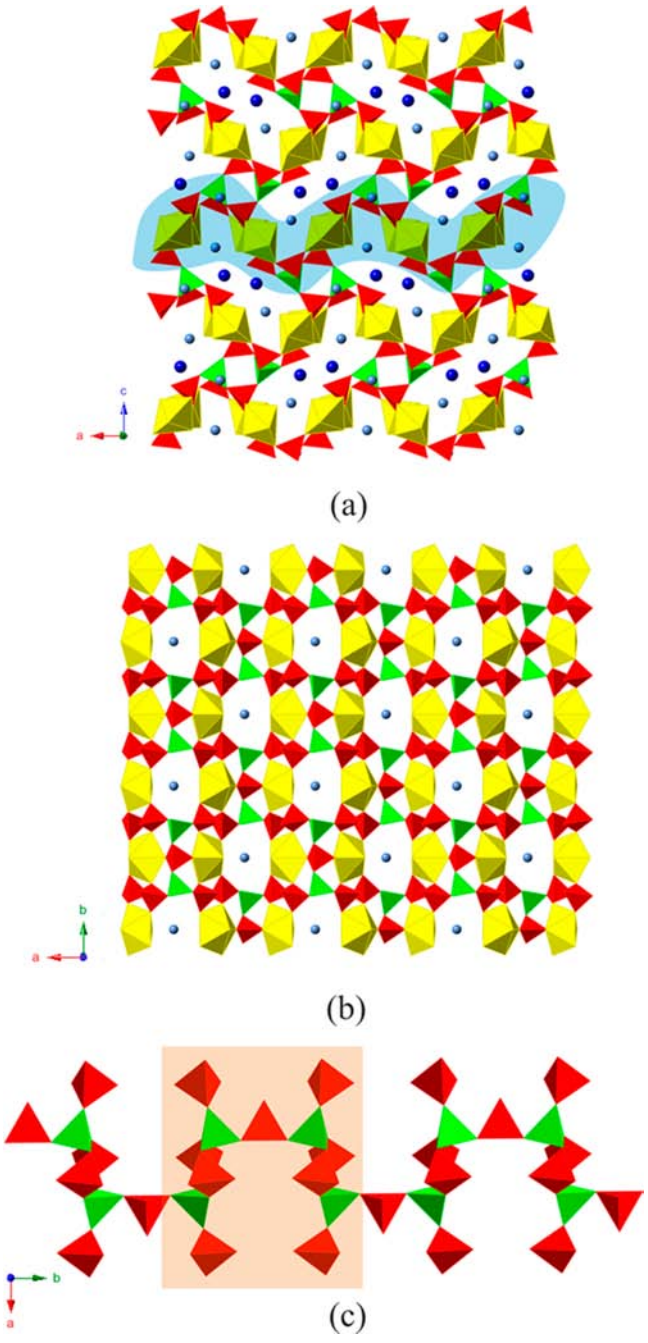

Figure 2. (a) Polyhedral view of the structure of **AgNBPU-2** and **AgNBPU-3** emphasizing the corrugated layers (marked in light blue). (b) Top view of the corrugated layers. (c) The borophosphate chains within the layers. UO_7 pentagonal bipyramids are shown in yellow, BO_4 tetrahedra are shown in green and PO_4 tetrahedra are shown in red. Ag atoms are shown in blue, and NH_4^+ groups are shown in pale blue spheres, respectively.

The framework in **AgNBPU-2** and **AgNBPU-3** has two types of the channels. The large one is parallel to *b*-axis as can be clearly seen in Figure 2a. This channel has a nearly elliptic 8.5 Å × 3 Å profile and is occupied by Ag^+ and NH_4^+ cations. The positions of the Ag atoms are partially occupied and split, with a ~ 0.87 Å distance between the split positions. The NH_4^+ groups have two crystallographic positions. One is within the large channel, and the second resides in a small zigzag-like channel composed by the layer-like fragment, as shown in Figure 2b.

3.3. Borophosphate Fundamental Building Blocks and Structure Topology. Numerous different fundamental buildings blocks (FBBs) are known from pure borates, borogermanates, borosilicates, and borophosphates.[1,2,36] The two FBBs observed in this work are new (Figure 3). The FFB

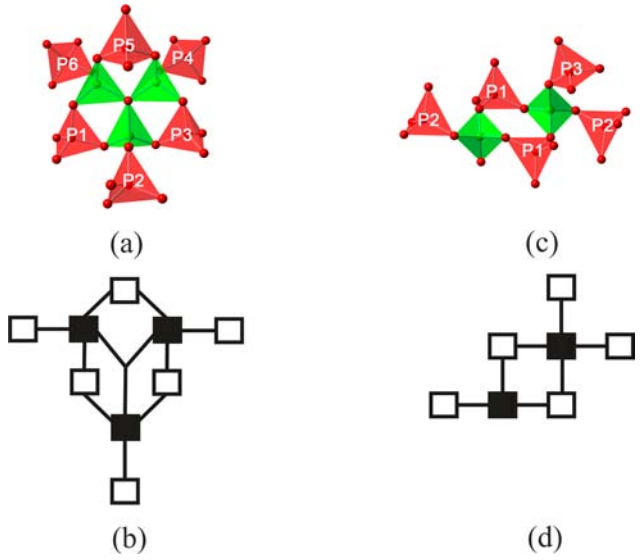

Figure 3. Fundamental building blocks and respective topologies in **AgNBPU-1** (a, b) and **AgNBPU-2, 3** (c, d). BO_4 tetrahedra are shown in green and black squares, and PO_4 tetrahedra are shown in red and white squares.

of **AgNBPU-1** is topologically identical with the finite borophosphate unit in the structure of $[B_3O(PO_4)_4(PO_4H)_2]$. This unit and its topological representation are shown in Figure 3a,b, respectively. It is based on nine tetrahedra, and all these polyhedra are linked by corner-sharing. The B/P ratio is 1:2, and the topology of the unit can be represented as a derivative of the simplest 3□:3□ FBB.[2] The $[B_3O(PO_4)_4(PO_4H)_2]$ is the first borophosphate FBB with μ_3 oxygen bridging BO_4 groups. The B_3O fragment is central to the FBB unit in **AgNBPU-1**. The topology of the FBB can be written as 9□: [Φ]□⟨3□⟩□|□⟨3□⟩□|□⟨3□⟩□| following Burns et al.'s designations.[36] Each FBB has a descriptor of the form A:B, where A gives the number of borate triangles (Δ) and tetrahedra (□) in the FBB in the form *i*Δ*j*□, where *i* and *j* are the numbers of triangles and tetrahedra, respectively. The delimiters, ⟨ ⟩ and [ ], are used to identify the rings of polyhedral and connected anions, polyhedra, or rings. The Φ means O^{2-} or OH^-, in this case it is O^{2-}. Symbols | are used to show one oxygen atom that is shared among different tetrahedra.[36] At present, the topology of this FBB is the most complex one ever found in the B:P = 1:2 group of borophosphates.

The FBB in **AgNBPU-2,3** phases is based on two BO_4 and five PO_4 groups (Figure 3c). This FBB can be separated from the $[B_2P_5O_{(20-x)}(OH)_x]_1$ chain and possesses a topology schematically shown in Figure 3d. This fragment is based on seven tetrahedra and can be represented by 7□:□⟨4□⟩□|□. This FBB is an isomer of two other FBBs with the same composition, 7□:[3□]□|□|□|□| and 7□: [⟨3□⟩]□|□|□|□|, observed in complex vanadyl borophos-

dx.doi.org/10.1021/ic400214x | *Inorg. Chem.* 2013, 52, 7881−7888

phates $(N_2C_3H_5)_{3.8}(H_3O)_{1.2}[(VO)_4B_2P_5O_{22}]\cdot 0.3H_2O$ and $(C_6H_{14}N_2)_2[VBP_5O_{17}(OH)_5]\cdot H_2O\cdot H_3PO_4$, respectively.[2,37] The FFB in **AgNBPU-2,3** is connected to a six-member FBB (6□:□⟨4□⟩□) directly and can be obtained from the latter by adding one PO_4 group.[2]

The topology of the layers (in the case of **AgNBPU-2,3** it is a quasilayer fragment) can be described with an anion topology method.[38] The black and white graphs for both structures are presented in Figure 4. The graph of **AgNBPU-1** consists of

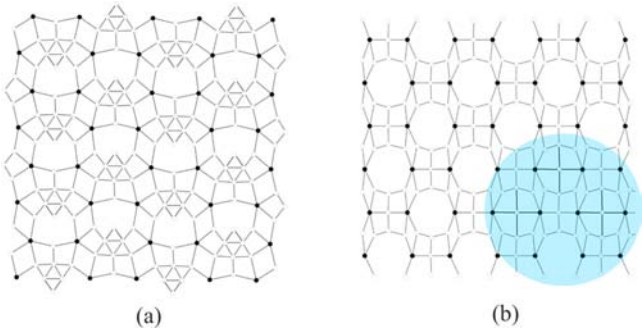

Figure 4. Anion topologies of **AgNBPU-1** (a) and **AgNBPU-2, 3** (b).

three-, four-, and eight-membered rings (Figure 4a) and can be written as $3^44^58^1$ in terms of ring symbols.[37] It is quite complicated to write a basic graph for the layers in **AgNBPU-1** because they are based on highly polymeric B−P units. This is the first time that such a topology has been observed in actinide phases. The topology of the quasilayers in **AgNBPU-2,3** is simpler as it is based on four- and eight-membered rings only (4^68^1). The topology of these layers can be derived from a {**6.3.4.4**}{**6.3.6.3**} basic graph via elimination of one white element from the center of the hole. The idealized graph is shown on the right bottom corner in Figure 4b (separated by light blue). Such a topology is new for the known actinide inorganic phases.

3.4. Specific Solid Solution. Our attempts to prepare a pure As analogue of **AgNBPU-2** were unsuccessful which possibly shows the instability of this potential phase. However, we successfully synthesized a P/As solid solution with the same crystalline structure. Our synthetic scheme was to use an equal molar ratio of both P and As in an attempt to substitute As for P. As a result, we got the **AgNBPU-3** in which the ideal P:As ratio is 1.25:1 which was calculated according to the site occupation factor (sof) of each atom. The presence of both P and As has been proved by the EDX data with a detected P:As ratio of 1.40:1 which is close to the ideal ratio obtained from refinement (Figure S6, Table S3). This result might indicate that the composition of this phase represents the upper limit of As substitution in this solid solution series. The structural study performed on single crystals demonstrates the quite interesting feature of P/As isomorphism. The T−O distances increase with the increasing substitution of As into the P sites as expected from the larger ionic radius of As. In Figure 5, a fragment of **AgNBPU-3** is shown which includes all crystallographic sites of B, P(As), and U atoms. From this picture one can see that one of the three possible P positions (P3) is fully occupied by P (red tetrahedron) which is same as that in **AgNBPU-2**. The full occupancy of P3 is confirmed by the BVS (Table S12). The bond lengths within the PO_4 tetrahedron are in the range 1.46(2)−1.58(2) Å which is similar to that of the pure end member **AgNBPU-2** (Table S8, Table S10). The other two sites are partially occupied by As based on the sof of each atom, viz. T1(P) 0.68, T1(As) 0.32, T2(P) 0.12, and T2(As) 0.80. However, the sof for both P1 and P2 in **AgNBPU-2** is 1. The BVS confirmed the presence of As at the T1 and T2 sites as is shown in Table S12.[31] The T1 site is 70% occupied by P atoms and only 30% by As. The bond lengths within this TO_4 group (T: P/As) are in the range 1.54(1)−1.60(1) Å which are longer than that in **AgNBPU-2** (1.515(4)−1.574(4) Å). The most significant incorporation of As occurs in the hydroxylated PO_3OH group around T2, where the P/As ratio is $^1/_4$. The bond lengths of T−O range from 1.63(1) to 1.68(1) Å which are much longer than those in **AgNBPU-2** (Table S8, Table S10). However, these T−O bond lengths are quite typical for As^{5+} oxo-tetrahedra.[21,39]

Obviously, As and P have distinct preferences for the three sites, which results in site occupancies that most likely depend on the As/P ratio during synthesis, but may also depend on pressure and temperature. This observation opens the possibility for a complex ordering scheme in this solid solution series. $T(1)O_4$ and $P(3)O_4$ are both fully connected with two BO_4 and two uranyl groups, whereas $T(2)O_4$ is connected with only one BO_4 and two uranyl groups while the fourth bond is T−OH. This loose coordination environment of T2 is arguably the reason why it is easier for this site to be substituted by the larger As for P, than in the more tightly connected tetrahedra

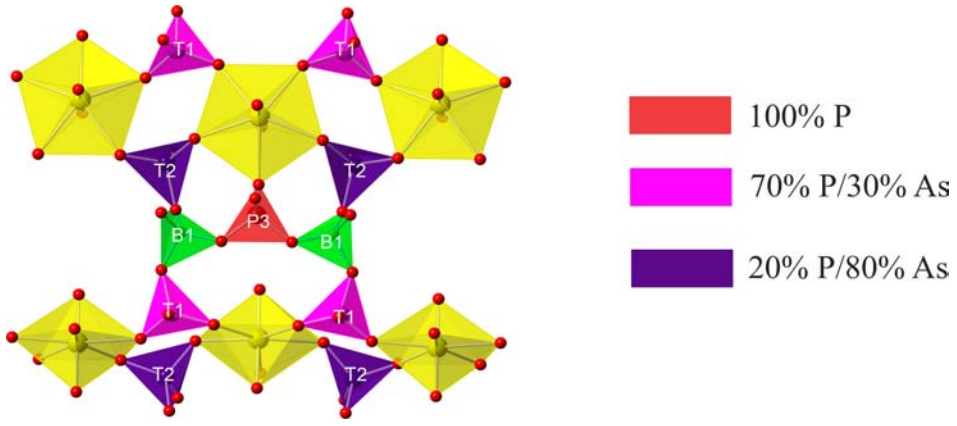

Figure 5. Crystallographic sites of B, P(As), and U atoms in **AgNBPU-3**. UO_7 pentagonal bipyramids are shown in yellow, BO_4 tetrahedra are shown in green, PO_4 tetrahedra are shown in red, and TO_4 (T = P, As) tetrahedra are shown in pink and purple.

dx.doi.org/10.1021/ic400214x | *Inorg. Chem.* 2013, 52, 7881−7888

around T1 and P3. In mineralogy, the occurrence of preference for distinct sites is a quite common phenomenon such as for the cation sites in pyroxenes, amphiboles, or tourmaline, and for the different T sites in the anionic partial structure of feldspars.

3.5. Spectroscopic Properties. Single crystal infrared spectroscopy clearly shows the presence of NH_4^+ in all three structures by the stretch observed between 1412 and 1427 cm^{-1} (Figure S8). The symmetric stretching vibrations (ν_1) of PO_4^{3-} were recorded at 967, 987, and 980 cm^{-1} for **AgNBPU-1**, **AgNBPU-2**, and **AgNBPU-3**, respectively, while the symmetric stretching vibrations of UO_2^{2+} were observed at around 878−892 cm^{-1}. The bands between 1036 and 1095 cm^{-1} were assigned to the antisymmetric stretching vibration (ν_3) of BO_4^{5-} and PO_4^{3-}. It is noteworthy that the broad bands between 2500 and 3600 cm^{-1} are contributed by both the stretching vibration νOH and νN−H. In **AgNBPU-1**, there is a peak at 1643 cm^{-1} which is identified as the stretching mode of the H_2O molecules present in the structures. Moreover, the presence of AsO_4^{3-} in **AgNBPU-3** is confirmed by the peak at 805 cm^{-1} which was assigned to the antisymmetric stretching vibration (ν_3) of AsO_4^{3-}. The strong peak at 1231 cm^{-1} in **AgNBPU-3** might be assigned to the symmetric stretching vibration of TO_4 (T = P, As) groups.[40]

Uranyl ion usually produces a vibrational-coupled electronic transition around 420 nm, which is attributed to a singlet−triplet transition between the HOMO and LUMO of $(UO_2)^{2+}$ molecular orbitals derived by the hybridization of uranium 5f and oxygen 2p orbitals.[41] The solid state UV−vis−NIR spectra of **AgNBPU-1**, **AgNBPU-2**, and **AgNBPU-3** are shown in Figure S9. All of three phases exhibit strong peaks at ∼350 nm and transition at ∼430 nm which is typical for U(VI) compounds such as $UO_2(NO_3)_2{\cdot}6H_2O$.[42] It is noteworthy that the peak at ∼430 nm for **AgNBPU-1** is much weaker compared with those for **AgNBPU-2** and **AgNBPU-3**.

Fluorescence from uranyl compounds can be identified from the vibronic fine-structure characteristic of the UO_2^{2+} moiety.[43] As shown in Figure S10, the solid state fluorescence spectra of **AgNBPU-1**, **AgNBPU-2**, and **AgNBPU-3** are centered near 520 nm which are consistent with other U(VI) compounds.[23a,b,42]

CONCLUSION

In conclusion, the H_3BO_3−$NH_4H_2PO_4$/$NH_4H_2AsO_4$ flux method was used to synthesize the first examples of actinide borophosphates which extend our knowledge of the borophosphate family. The two new fundamental building blocks (FBBs) of borophosphate observed in **AgNBPU-1** and **AgNBPU-2,3** provide unprecedented structural types in borophosphate chemistry. The new finding demonstrates the flexibility of the B−P systems. Furthermore, the discovery of these uranyl borophosphates lends itself to the idea that the formation of crystalline actinide borophosphates might be possible during the corrosion of the borophosphate nuclear waste glasses.

ASSOCIATED CONTENT

Supporting Information

FT-IR, UV−vis−NIR, SEM−EDX, selected bond distances, angles, bond valence sum (BVS), and X-ray files (cif) for $Ag_2(NH_4)_3[(UO_2)_2\{B_3O(PO_4)_4(PO_4H)_2\}]H_2O$ (**AgNBPU-1**), $Ag_{(2-x)}(NH_4)_3[(UO_2)_2\{B_2P_5O_{(20-x)}(OH)_x\}]$ (x = 1.26) (**AgNBPU-2**), and $Ag_{(2-x)}(NH_4)_3[(UO_2)_2\{B_2P_{(5-y)}As_yO_{(20-x)}(OH)_x\}]$ (x = 1.43, y = 2.24) (**AgNBPU-3**), and DSC data for **AgNBPU-3**. This material is available free of charge via the Internet at http://pubs.acs.org.

AUTHOR INFORMATION

Corresponding Author

*E-mail: albrecht-schmitt@chem.fsu.edu (T.E.A.-S.); e.alekseev@fz-juelich.de (E.V.A.).

Author Contributions

All authors have given approval to the final version of the manuscript.

Notes

The authors declare no competing financial interest.

ACKNOWLEDGMENTS

We are grateful for the support provided by Deutsche Forschungsgemeinschaft (DE 412/43-1), Chemical Sciences, Geosciences, and Biosciences Division, Office of Basic Energy Sciences, Office of Science, Heavy Elements Program, U.S. Department of Energy (DE-SC0002215), Helmholtz Association (VH-NG-815), and National Natural Sciences Foundation of China (41103055).

REFERENCES

(1) Kniep, R.; Engelhardt, H.; Hauf, C. *Chem. Mater.* **1998**, *10* (10), 2930−2934.

(2) Ewald, B.; Huang, Y.-X.; Kniep, R. *Z. Anorg. Allg. Chem.* **2007**, *633* (10), 1517−1540.

(3) (a) Noellner, C. *Münch Akad. Ber.* **1870**, 291−293. (b) Gupta, P. K. S.; Swihart, G. H.; Dimitrijevic, R.; Hossain, M. B. *Am. Mineral.* **1991**, *76* (7−8), 1400−1407.

(4) (a) Kraus, E. H.; Seaman, W. A.; Slawson, C. B. *Am. Mineral.* **1930**, *15* (6), 220−225. (b) Moore, P. B.; Ghose, S. *Am. Mineral.* **1971**, *56* (9−10), 1527−1538.

(5) Sokolova, E.; Hawthorne, F. C.; Pautov, L. A.; Agakhanov, A. A. *Mineral. Mag.* **2010**, *74* (2), 285−308.

(6) Raade, G.; Grice, J. D.; Erambert, M.; Kristiansson, P.; Witzke, T. *Mineral. Mag.* **2008**, *72* (5), 1071−1082.

(7) Raade, G.; Johnsen, O.; Erambert, M.; Petersen, O. V. *Mineral. Mag.* **2007**, *71* (2), 179−192.

(8) Boiocchi, M.; Callegari, A.; Ottolini, L.; Maras, A. *Am. Mineral.* **2004**, *89*, 1540−1545.

(9) Maras, A.; Parodi, G. C.; Della Ventura, G.; Ohnenstetter, D. *Eur. J. Mineral.* **1995**, *7* (2), 439−446.

(10) Vogel, V. *Z. Anal. Chem.* **1870**, 376.

(11) Kniep, R.; Gozel, G.; Eisenmann, B.; Rohr, C.; Asbrand, M.; Kizilyalli, M. *Angew. Chem., Int. Ed.* **1994**, *33* (7), 749−751.

(12) Vogel, J.; Wange, P.; Hartmann, P. *Glastech. Ber.* **1997**, *70* (7), 220−223.

(13) Shah, K. V.; Goswami, M.; Deo, M. N.; Sarkar, A.; Manikandan, S.; Shrikhande, V. K.; Kothiyal, G. P. *Bull. Mater. Sci.* **2006**, *29* (1), 43−48.

(14) Liang, W.; Cheng, J. J.; Wang, H. P.; Luo, H. *Phys. Chem. Glasses* **2002**, *43* (3), 158−160.

(15) Nazabal, V.; Fargin, E.; Labrugere, C.; Le Flem, G. *J. Non-Cryst. Solids* **2000**, *270* (1−3), 223−233.

(16) (a) International Atomic Energy Agency. *Spent Fuel and High Level Waste: Chemical Durability and Performance under Simulated Repository Conditions*; International Atomic Energy Agency: Vienna, 2007. (b) Commission on Geosciences, Envrionment and Resources. *Glass as a Waste Form and Vitrification Technology: Summary of an International Workshop*; National Academy of Science: Washington, DC, 1996.

(17) (a) Werme, L.; Bjorner, I. K.; Bart, G.; Zwicky, H. U.; Grambow, B.; Lutze, W.; Ewing, R. C.; Magrabi, C. *J. Mater. Res.* **1990**, *5* (5), 1130−1146. (b) Vernaz, E. Y.; Dussossoy, J. L. *Appl. Geochem.*

1992, No. Suppl. 1, 13−22. (c) Abdelouas, A.; Crovisier, J. L.; Lutze, W.; Grambow, B.; Dran, J. C.; Muller, R. *J. Nucl. Mater.* **1997**, *240* (2), 100−111. (d) Grambow, B. *Elements* **2006**, *2* (6), 357−364.

(18) (a) Burns, P. C. *Can. Mineral.* **2005**, *43*, 1839−1894. (b) Hazen, R. M.; Ewing, R. C.; Sverjensky, D. A. *Am. Mineral.* **2009**, *94* (10), 1293−1311.

(19) Rey, A.; Gimenez, J.; Casas, I.; Clarens, F.; de Pablo, J. *Appl. Geochem.* **2008**, *23* (8), 2249−2255.

(20) (a) Alekseev, E. V.; Krivovichev, S. V.; Depmeier, W.; Knorr, K. *Z. Anorg. Allg. Chem.* **2008**, *634* (9), 1527−1532. (b) Alekseev, E. V.; Krivovichev, S. V.; Depmeier, W. *J. Solid State Chem.* **2009**, *182* (11), 2977−2984. (c) Forbes, T. Z.; Burns, P. C. *Am. Mineral.* **2006**, *91* (7), 1089−1093. (d) Locock, A. J.; Burns, P. C. *J. Solid State Chem.* **2002**, *167* (1), 226−236. (e) Locock, A. J.; Burns, P. C. *J. Solid State Chem.* **2003**, *175* (2), 372−379. (f) Forbes, T. Z.; Burns, P. C. *Can. Mineral.* **2007**, *45*, 471−477.

(21) (a) Alekseev, E. V.; Krivovichev, S. V.; Malcherek, T.; Depmeier, W. *J. Solid State Chem.* **2008**, *181* (11), 3010−3015. (b) Alekseev, E. V.; Krivovichev, S. V.; Depmeier, W. *J. Solid State Chem.* **2009**, *182* (8), 2074−2080.

(22) (a) Wang, S.; Alekseev, E. V.; Juan, D. W.; Casey, W. H.; Phillips, B. L.; Depmeier, W.; Albrecht-Schmitt, T. E. *Angew. Chem., Int. Ed.* **2010**, *49* (6), 1057−1060. (b) Wang, S.; Alekseev, E. V.; Ling, J.; Skanthakumar, S.; Soderholm, L.; Depmeier, W.; Albrecht-Schmitt, T. E. *Angew. Chem., Int. Ed.* **2010**, *49* (7), 1263−1266. (c) Wang, S.; Alekseev, E. V.; Depmeier, W.; Albrecht-Schmitt, T. E. *Inorg. Chem.* **2011**, *50* (6), 2079−2081. (d) Polinski, M. J.; Wang, S.; Alekseev, E. V.; Depmeier, W.; Albrecht-Schmitt, T. E. *Angew. Chem., Int. Ed.* **2011**, *50* (38), 8891−8894. (e) Polinski, M. J.; Wang, S.; Alekseev, E. V.; Depmeier, W.; Liu, G.; Haire, R. G.; Albrecht-Schmitt, T. E. *Angew. Chem., Int. Ed.* **2012**, *51* (8), 1869−1872. (f) Polinski, M. J.; Grant, D. J.; Wang, S.; Alekseev, E. V.; Cross, J. N.; Villa, E. M.; Depmeier, W.; Gagliardi, L.; Albrecht-Schmitt, T. E. *J. Am. Chem. Soc.* **2012**, *134* (25), 10682−10692. (g) Polinski, M. J.; Wang, S.; Cross, J. N.; Alekseev, E. V.; Depmeier, W.; Albrecht-Schmitt, T. E. *Inorg. Chem.* **2012**, *51* (14), 7859−7866.

(23) (a) Wang, S.; Alekseev, E. V.; Stritzinger, J. T.; Depmeier, W.; Albrecht-Schmitt, T. E. *Inorg. Chem.* **2010**, *49* (14), 6690−6696. (b) Wang, S.; Alekseev, E. V.; Stritzinger, J. T.; Liu, G. K.; Depmeier, W.; Albrecht-Schmitt, T. E. *Chem. Mater.* **2010**, *22* (21), 5983−5991. (c) Wang, S.; Alekseev, E. V.; Ling, J.; Liu, G. K.; Depmeier, W.; Albrecht-Schmitt, T. E. *Chem. Mater.* **2010**, *22* (6), 2155−2163.

(24) Lipp, C.; Burns, P. C. *Can. Mineral.* **2011**, *49* (5), 1211−1220.

(25) Wu, S.; Wang, S.; Diwu, J.; Depmeier, W.; Malcherek, T.; Alekseev, E. V.; Albrecht-Schmitt, T. E. *Chem. Commun.* **2012**, *48* (29), 2334−2336.

(26) Duisenberg, A, J. M.; Kroon-Batenburg, L. M. J.; Schreurs, A. M. M. *J. Appl. Crystallogr.* **2003**, *36*, 220−229.

(27) (a) Sheldrick G. M. *SADABS, Program for Absorption Correction Using SMART CCD Based on the Method of Blessing*; 2001. (b) Blessing, R. H. *Acta Crystallogr.* **1995**, *A51*, 33−38.

(28) Sheldrick, G. M. *Acta Crystallogr.* **2008**, *A64*, 112−122.

(29) (a) Wang, Y.; Pan, S.; Shi, Y. *Chem.—Eur. J.* **2012**, *18* (38), 12046−12051. (b) Zhu, J.; Cheng, W.-D.; Wu, D.-S.; Zhang, H.; Gong, Y.-J.; Tong, H.-N.; Zhao, D. *Inorg. Chem.* **2007**, *46* (1), 208−212.

(30) Pan, S. L.; Wu, Y. C.; Fu, P. Z.; Wang, G. F.; Zhang, G. C.; Li, Z. H.; Chen, C. T. *Chem. Lett.* **2001**, No. 7, 628−629.

(31) (a) Brese, N. E.; Okeeffe, M. *Acta Crystallogr.* **1991**, *B47*, 192−197. (b) Burns, P. C.; Ewing, R. C.; Hawthorne, F. C. *Can. Mineral.* **1997**, *35*, 1551−1570.

(32) Heymann, G.; Soltner, T.; Huppertz, H. *Solid State Sci.* **2006**, *8* (7), 821−829.

(33) Harmon, S. B.; Sevov, S. C. *Chem. Mater.* **1998**, *10* (10), 3020−3023.

(34) Fox, B. S.; Beyer, M. K.; Bondybey, V. E. *J. Am. Chem. Soc.* **2002**, *124*, 13613−13623.

(35) (a) Yaghi, O. M.; Li, H. *J. Am. Chem. Soc.* **1996**, *118*, 295−296. (b) Zhang, Y.; Wang, H.; Liu, J.; Wang, Y.; Fu, A.; Shi, Q. *Inorg. Chem. Commun.* **2009**, *12*, 611−614.

(36) Burns, P. C. *Can. Mineral.* **1995**, *33*, 1131−1151.

(37) (a) Bontchev, R. P.; Do, J.; Jacobson, A. J. *Inorg. Chem.* **2000**, *39* (15), 3320−3324. (b) Wikstad, E.; Kritikos, M. *Acta Crystallogr.* **2003**, *C59*, m87−m89.

(38) Krivovichev, S. V.; Burns, P. C.; Tananaev, I. G. *Structural Chemistry of Inorganic Actinide Compounds*; Elsevier: New York, 2007.

(39) (a) Alekseev, E. V.; Krivovichev, S. V.; Depmeier, W. *Z. Anorg. Allg. Chem.* **2007**, *633* (8), 1125−1126. (b) Alekseev, E. V.; Krivovichev, S. V.; Depmeier, W. *J. Mater. Chem.* **2009**, *19* (17), 2583−2587. (c) Alekseev, E. V.; Krivovichev, S. V.; Depmeier, W. *Cryst. Growth Des.* **2011**, *11* (7), 3295−3300.

(40) (a) Čejka, J. Infrared spectroscopy and thermal analysis of the uranyl minerals. *Uranium: Mineralogy, Geochmistry and the Environment*; Burns, P. C., Finch, R., Eds.; Reviews in Mineralogy; Mineralogical Society of America: Chantilly, VA, 1999; Vol. *38*, pp 521−622. (b) Baykal, A.; Kizilyalli, M.; Kniep, R. *J. Mater. Sci.* **2000**, *35*, 4621−4626. (c) Stuart, B. *Spetroscopy: Fundamentals and Applications*; John Wiley & Sons, Ltd.: New York, 2004. (d) Yakubovich, O, V.; Steele, I. M.; Atencio, D.; Menezes, L, A.; Chukanov, N. V. *Crystallogr. Rep.* **2008**, *53*, 764−770.

(41) (a) Meinrath, G. *J. Radioanal. Nucl. Chem.* **1997**, *224*, 119−126. (b) Jeżowska-Trzebiatowska, B.; Bartecki, A. *Spectrochim. Acta* **1962**, *18*, 799−807. (c) Brint, P.; McCaffery, A. *J. Mol. Phys.* **1973**, *25*, 311−322. (d) McGlynn, S. P.; Smith, J. K. *J. Mol. Spectrosc.* **1961**, *6*, 164−187.

(42) Weng, Z. H.; Wang, S.; Ling, J.; Morrison, J. M.; Burns, P. C. *Inorg. Chem.* **2012**, *51* (13), 7185−7191.

(43) Denning, R. G.; Norris, J. O. W.; Short, I. G.; Snellgrove, T. R.; Woodwark, D. R. *Lanthanide and Actinide Chemistry and Spectroscopy*; Edelstein, N. M., Ed.; ACS Symposium Series 131; American Chemical Society: Washington, DC, 1980; Chapter 15.